PHYSICAL REVIEW B VOLUME 34, NUMBER 5 1 SEPTEMBER 1986

Superconductivity in sulfur-based organic superconductors: A volume property

H. Schwenk,[*] S. S. P. Parkin, V. Y. Lee, and R. L. Greene[†]
IBM Almaden Research Center, 650 Harry Road, San Jose, California 65120-6099

(Received 6 September 1985; revised manuscript received 18 June 1986)

We have shown by dc low-field magnetization measurements the existence of diamagnetic shielding and Meissner signals in the ambient-pressure organic superconductors, β-$(ET)_2IBr_2$ and β-$(ET)_2AuI_2$, below $T=2.5$ K and $T=4.1$ K, respectively [ET is bis(ethylenedithio)tetrathiafulvalene]. This proves that superconductivity is a volume property in these compounds. We also measured the upper critical field H_{c2} in the compound β-$(ET)_2AuI_2$. Combined with the low-data this yields a thermodynamically consistent picture using Ginzburg-Landau theory and a weak-coupling Bardeen-Cooper-Schrieffer gap.

I. INTRODUCTION

The search for new superconducting organic molecular crystals is presently focused on compounds based on the cation bis(ethylenedithio)tetrathiafulvalene (ET), since these appear to be the most promising candidates in which to obtain superconducting transition temperatures as high as possibly 10 K.[1] Historically the first sulphur-based organic superconductor was $(ET)_2ReO_4$ with T_c below $\simeq 2$ K for pressures exceeding $P_c \simeq 4$ kbar.[2] Ambient-pressure superconductivity was subsequently observed in compounds with linear anions consisting of three atoms of which at least one is iodine: various phases have been studied including $\beta(ET)_2I_3$, $T_c=1.4$ K;[3] β-$(ET)_2IBr_2$, $T_c=2.5$ K;[4] and β-ET_2AuI_2, $T_c=4.3$ K.[5] The most fascinating result, however, has been the observation of superconductivity at $T_c=8$ K in β-$(ET)_2I_3$ (Refs. 6–8) when a low pressure of 1.3 kbar is applied, and—only recently—the stabilization of an 8-K ambient-pressure superconducting phase in the same compound, when the pressure of 1.5 kbar, applied at room temperature, is released below 100 K.[9,10]

So far, high-temperature superconductivity has always been observed in materials where d and f bands have been involved. The occurrence of relatively high T_c's in the family of ET compounds where p bands dominate the electron transport is another most interesting facet of them.

In this paper we present low-field magnetization measurements at ambient pressure for β-$(ET)_2IBr_2$ and β-$(ET)_2AuI_2$. Via the observation of the Meissner effect we conclude the existence of bulk superconductivity in the two compounds, as has been done for β-$(ET)_2I_3$ (Refs. 8 and 11) below 1.4 K. Since the submission of this paper an independent study of the Meissner effect in the IBr_2 and AuI_2 compounds has been published[12] which is in complete agreement with the Meissner results we present here. The information about the bulk nature, in contrast to a possible filamentary nature of the superconducting state, is a necessary precondition for comparing experimental data, such as the upper critical field, with the appropriate theories. In addition, the knowledge about the superconducting volume fraction is a powerful criterion in the quality control of the electrochemically grown crystals, and thus for the improvement of the growth conditions. Furthermore, in this paper we will analyze the measured lower and upper critical fields of the two before-mentioned compounds within the Ginzburg-Landau theory, in order to investigate the thermodynamical consistency of our data. This is important, since in conjunction with other experiments, e.g., tunnelling, the detailed origin of the interaction which causes the superconductivity in the ET compounds can, in principle, be determined.

II. EXPERIMENTAL

All the ET_2X crystals were obtained by the electrochemical oxidation of ET (0.1 mM) in the presence of an appropriate electrolyte (0.02 M) solution. Electrolytes n-$Bu_4NH_4+X^-$ (where $X^+=I_3^-$, IBr_2^-, and AuI_2^-) were prepared following literature procedures.[13,14] Chlorobenzene was used as the solvent for growing $(ET)_2I_3$ crystals yielding both needles and distorted hexagon shapes. Another solvent, 1,2-dimethoxyethane, was employed for the production of (ET)-IBr_2 and (ET)-AuI_2 complexes. Typically two or more phases of these complexes were obtained on the platinum electrodes under constant current ($1-2\ \mu A$) conditions. In the case of $(ET)_2I_3$ the ESR linewidth (Γ) has been proposed as a means of experimentally distinguishing between α- and β-phase crystals: values of $\Gamma=20-25$ Oe have been reported for the β phase. We found similar linewidths for the superconducting β phases of $(ET)_2IBr_2$ and $(ET)_2AuI_2$, whereas, for example, the ESR linewidth of a semiconducting phase of $(ET)_2IBr_2$ was $\simeq 40$ Oe. By means of a four-circle x-ray diffractometer we could subsequently confirm that our samples were indeed of the β phase—through reproduction of the literature values of the unit cell parameters—as well as relate the morphology of our samples to specific crystallographic directions. Most important is the identification of the a-b plane, the plane of the sheets of organic molecules. In the direction perpendicular to the a-b plane, sheets of ET molecules are separated from each other by sheets of anions X.

The setup for the low-field magnetization measurements basically consisted of a pair of astatic coils—wound from 70 turns of 0.005-in. Nb wire of 1.4 mm diameter—in one of which the sample was placed. Flux changes in these pickup coils were detected with a superconducting quantum interference device. A static field was applied to the samples by a small superconducting solenoid. A permalloy shield on the outside of the cryostat reduced the residual fields to $\simeq 4$ mOe. The ensemble of pickup coils, field coil, thermometers, and heaters was attached to the mixing chamber of a dilution refrigerator. The sample (typically of size $0.5\times0.5\times0.2$ mm^3) was thermally anchored to the mixing chamber via a well-defined thermal link (0.1-mm-diam. Cu wire) so that it could be heated to 8 K, while the other parts of the ensemble remained at a fairly constant temperature. Magnetization signals were monitored at constant fields as a function of temperature and were calibrated against a Pb (99.999%) sample for which we assumed complete diamagnetism ($m = H/4\pi$).

Resistance measurements of our samples were carried out with the normal four-probe low-frequency lock-in technique; 0.0005-in. Au wires were glued to the sample with Au paint. Ac-susceptibility measurements were also performed in order to obtain the upper critical field, H_{c2} of β-$(\text{ET})_2\text{AuI}_2$. The change of the real part of the ac susceptibility—when the sample becomes superconducting—was detected via a shift in the resonance frequency of a parallel LC circuit. This circuit was biased close to its resonance frequency at 44.7 kHz with a constant current, and the change in the resonant frequency was monitored via the change in the voltage appearing across the resonant circuit with a lock-in detector. The ac field (typically $H_{\text{ac}} < 0.1$ Oe) was always parallel to the a-b plane. The angular alignment of the sample with respect to the dc field (of a superconducting magnet) was better than 2°. Samples were cooled in all runs at less than 1 K/min from 300 to 4 K.

III. RESULTS

dc-magnetization curves of the superconducting transition of β-$(\text{ET})_2\text{IBr}_2$ for a magnetic field of $H = 100$ mOe applied perpendicular to the highly conducting a-b plane ($\mathbf{H}\|\mathbf{c}^*$) are shown in the inset to Fig. 1. These curves are obtained in the following way: first the sample is cooled in zero field to well below T_c; then a dc field is applied which induces supercurrents at the sample surface within a layer of thickness equal to the penetration depth, so screening the magnetic field from the inside of the sample. Upon subsequent warming of the sample above T_c these supercurrents decay, resulting in a change in the magnetization: the diamagnetic shielding signal m_{dia}. Cooling back below T_c in the very same magnetic field leads to the formation of quantized flux lines in the bulk of the sample and their expulsion out of the sample: the Meissner effect. Therefore, it is the Meissner magnetization, m_{Meissner}, rather than m_{dia} that yields information on the bulk nature of the superconductivity (provided that m_{dia} exhibits a considerable fraction of complete diamagnetism). Note, however, that the pinning of flux lines at impurity sites or crystal defects will lead to some reduction of m_{Meissner} compared to m_{dia}. For example, m_{Meissner} ranges from 2—60% of m_{dia} in the organic superconductors, $(\text{TMTSeF})_2\text{ClO}_4$ (Ref. 15) and β-$(\text{ET})_2\text{I}_3$ (Ref. 11), for various field orientations. The superconducting transition temperature was defined by extrapolation of the linear part of the transition to $m = 0$.

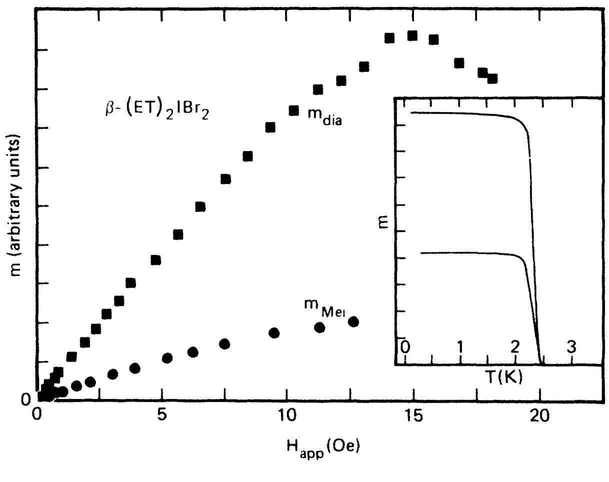

FIG. 1. Magnetization curves of the diamagnetic shielding (m_{dia}) and Meissner signal (m_{Meissner}) versus applied field ($\perp a$-b plane) at $T = 0.5$ K of β-$(\text{ET})_2\text{IBr}_2$. The inset shows the temperature dependence of the diamagnetic shielding and Meissner magnetization in an applied field of $H_{\perp ab} = 100$ mOe.

A. β-$(\text{ET})_2\text{IBr}_2$

T_c of our sample, as determined from m_{dia} in small magnetic fields (100 mOe, perpendicular to the a-b plane, for the data shown in the inset to Fig. 1) was 2.42 ± 0.05 K (with a transition width of 0.15 K), which compares well with values previously reported from measurements of the ac susceptibility[4] and resistivity[16]. Magnetization curves, m_{diam} and m_{Meissner}, for the field oriented perpendicular to the a-b plane at $T = 0.5$ K are shown in Fig. 1 and exhibit the typical type-III behavior found in all known organic superconductors. Values of the Meissner effect ($m_{\text{Meissner}}/m_{\text{dia}}$) and diamagnetic shielding magnetization in a small magnetic field ($H = 100$ mOe) as well as the lower critical field H_{c1} at $T = 0.5$ K for two orientations $\mathbf{H}\perp ab$ and $\mathbf{H}\|(110)$ are summarized in Table I. The large uncertainty in the data of m_{dia} results from the difficulties in measuring the sample volume accurately and in calculating the demagnetization coefficients, which requires approximating the sample shape by an ellipsoid. The latter problem also affects the derivation of the lower critical field, H_{c1}, i.e., its correction due to demagnetization effects. H_{c1} is defined as the field where the flux first starts to penetrate into the sample and thus corresponds to the first deviation from linearity in the magnetization curve of the diamagnetic shielding signal. (This field might be slightly enhanced above its thermodynamic value by flux pinning.)

TABLE I. Values of the initial diamagnetic shielding magnetization m_{dia} as a fraction of a complete diamagnetic shielding ($m_c=-H/4\pi$), the relative low-field Meissner magnetization ($m_{\text{Meissner}}/m_{\text{dia}}$), and the lower critical field H_{c1} of β-$(\text{ET})_2\text{IBr}_2$ at $T=0.5$ K and β-$(\text{ET})_2\text{AuI}_2$ at $T=1.2$ K. Values are corrected for demagnetization effects.

	β-$(\text{ET})_2\text{IBr}_2$		β-$(\text{ET})_2\text{AuI}_2$	
	H$\perp ab$	**H**$\parallel$(110)	**H**$\perp ab$	**H**$\parallel$**a**
m_{dia}/m_c (%)	80±20	80±20	80±20	80±20
$m_{\text{Meissner}}/m_{\text{dia}}$ (%)	47	22	55	25
H_{c1} (Oe)	16.5±3	3.9±1	20.5±2.8	4±1

B. β-$(\text{ET})_2\text{AuI}_2$

Figure 2 shows various transition curves determined from measurements of the resistivity ρ, ac susceptibility χ_{ac} (H_{ac} parallel to the a-b plane), diamagnetic shielding, and Meissner magnetizations (H perpendicular to the a-b plane). The data for ρ and χ_{ac} were taken on the same sample in consecutive runs. Thermal cycling of the sample did not affect the transition temperature. The onset of the magnetically detected transitions varied a little from sample to sample ($T_c=4.02$ to 4.2 K) but matched the temperature where the first superconducting path through the sample was completed, as inferred from the resistive transitions. Values of m_{dia}, m_{Meissner}, and H_{c1} at 1.2 K are presented in Table I. The upper critical fields—as derived from the ac susceptibility—for H parallel to the a axis and H perpendicular to the a-b plane are shown in Fig. 3 as a function of temperature. The zero-temperature values of the upper critical fields may be estimated by linear extrapolation as $H_{c2\perp ab}(0)=5.1$ kG and $H_{c2,\parallel a}(0)=66.3$ kG with an anisotropy parameter $\epsilon=H_{c2,\perp}/H_{c2,\parallel}=0.077$.

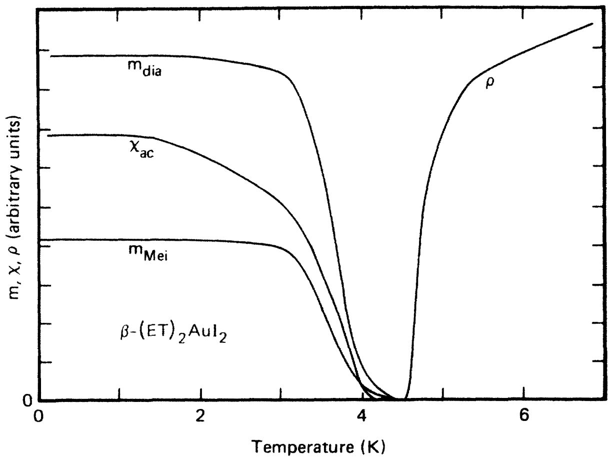

FIG. 2. Various superconducting transition curves of β-$(\text{ET})_2\text{AuI}_2$: Diamagnetic shielding m_{dia} and Meissner magnetization, m_{Meissner} were taken in an applied field, $H_{\perp ab}=100$ mG; ac susceptibility χ_{ac} and resistivity ρ, were taken on the same sample in successive runs in zero magnetic field.

C. β-$(\text{ET})_2\text{I}_3$

At ambient pressure we observed no diamagnetic shielding magnetization in β-$(\text{ET})_2\text{I}_3$ between 1.4 and 8 K to a resolution of 0.05% of m_{dia} of the signal below 1.4 K on samples which were pressure cycled at room temperature. Our pressure-cycled samples had, at ambient pressure, a complete resistive superconducting transition below 8 K as earlier reported by Tokumoto *et al.*[17] Since the submission of this paper, the reason for our observation of the lack of bulk superconductivity between 1.4 and 8 K has become clear. Recent work[9,10] has shown that the 8-K superconductivity comes from a metastable phase of β-$(\text{ET})_2\text{I}_3$ which is only stable below ~120 K at ambient pressure.

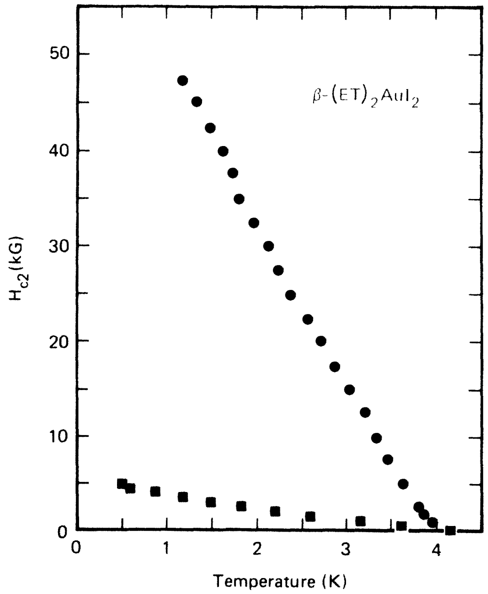

FIG. 3. Temperature dependence of the upper critical field H_{c2}, as determined from the ac susceptibility of β-$(\text{ET})_2\text{AuI}_2$, for fields applied perpendicular to the a-b plane (□) and parallel to the a axis (○).

IV. DISCUSSION

The existence of nearly complete diamagnetic shielding currents at the sample surface and a considerable Meissner effect, which has independently been observed by Heidmann *et al.*,[12] proves that superconductivity in both β-(ET)$_2$IBr$_2$ and β-(ET)$_2$AuI$_2$ is a bulk phenomenon, as it is in β-(ET)$_2$I$_3$ at ambient pressure below 1.4 K (Ref. 11) and below 6.5 K when a moderate pressure of 1.5 kbar is applied.[8] Crystals of the isostructural β-(ET)$_2X$ salts ($X = I_3$, IBr$_2$, AuI$_2$) behave similarly at low temperatures. In particular, they are all volume superconductors (with $T_c = 1.4$, 2.4, and 4.1 K, respectively) and all exhibit a considerable anisotropy of their superconducting properties along directions perpendicular and parallel to the *a-b* plane (for example, $H_{c2,\perp}/H_{c2,\parallel} = 0.007$ in the AuI$_2$ compound). In contrast, only a very small in-plane anisotropy has been reported in the I$_3$ and IBr$_2$ compounds.[16,18,19] Although we did not investigate the in-plane anisotropy of the AuI$_2$ salt, we shall assume that it too is negligible, for the purpose of the analysis of our data according to the anisotropic effective-mass model within the Ginzburg-Landau theory. This theory has quite successfully been applied to the class of layered-structure-type superconductors (transition-metal dichalcogenides).[20] The superconducting members of the ET family, when compared to the above-mentioned layered compounds, behave very similarly e.g., with respect to their structural and superconducting properties.

To start a detailed discussion of our experimental data, it is worthwhile to compare the different temperature behaviors of the magnetically and resistively monitored transition curves of β-(ET)$_2$AuI$_2$ in Fig. 2. The resistivity ρ, and ac susceptibility χ_{ac} were measured on the same sample, in consecutive runs. However, the onset of the resistive transition is around 5.5 K and it is completed at 4.6 K, exactly at the temperature where the magnetic transition has its onset (from an extrapolation of the linear part of the transition to zero, one obtains a value of 4.05 K—which, by definition, is the transition temperature T_c). This pronounced difference in the two types of transition curves has also been observed earlier in other organic superconductors, such as in (TMTSF)$_2$ClO$_4$,[21] and may be explained in the following way. The two above-mentioned experimental methods probe different parts of the sample. In order to observe a drop to zero of the electrical resistance, it is sufficient that a single superconducting path is developing in the sample between the potential leads, i.e., several superconducting regions are connected together. This way, the measurement of the electrical resistance is a powerful tool for observing even traces of superconductivity. A detection of a comparable signal of the ac susceptibility or diamagnetic shielding magnetization (dc signal), however, requires a closed loop of connected superconducting regions in the sample, or—as usually is in volume superconductors—on the surface of the sample within a layer of the thickness of the penetration depth. Thus, the development of a single path somewhere in the sample between the potential leads (in order to detect superconductivity in the resistivity experiment) will happen at higher temperatures than the development of a superconducting loop on the surface (in order to monitor a signal in an ac-susceptibility or diamagnetic shielding experiment), especially in materials with a T_c distribution of considerable width in the sample, such as the organic superconductors.

The transition curves of the ac susceptibility and the diamagnetic shielding magnetization (dc signal) are rather similar, except that the former is broadened, compared to the latter. This is due to the fact that the ac field has been oriented parallel to the *a-b* plane, whereas the dc field was perpendicular to it. When the field in the dc experiment is also applied parallel to the crystallographic *a-b* plane (curve not shown in Fig. 2), the transition is broadened exactly in the same way it is in the ac-susceptibility experiment with $\mathbf{H}\parallel a$-b plane. This behavior of a broadened transition, when the field is applied parallel to the *a-b* plane instead of perpendicular to it, is explained by the anisotropy of the London penetration depth and the fact that it is macroscopically large for a field oriented perpendicular to the *a-b* plane. Such a macroscopically large London penetration depth had previously been observed in the organic superconductor (TMTSF)$_2$ClO$_4$ for a certain field orientation.[15,22] In the family of ET compounds, the effective mass is largest for electrons moving perpendicular to the *a-b* plane, because the interactions between the sheets of ET molecules are weaker than the inter- and intrastack interactions within the *a-b* plane. When the field is oriented in the *a-b* plane, e.g., along the *a* direction, then the diamagnetic screening currents will flow in the plane perpendicular to *a*, in the $\mathbf{b}^*$-$\mathbf{c}^*$ plane. The electrons then have their biggest effective mass while they move perpendicular to the *a-b* plane, i.e., when they move along $\mathbf{c}^*$. This big effective mass causes a large penetration depth for the field oriented along a, penetrating along $\mathbf{b}^*$. This penetration depth, for a field oriented in the *a-b* plane, and penetrating also in the plane but in a direction perpendicular to the applied field, is denoted as $\lambda_\perp$. Its value for β-(ET)$_2$AuI$_2$ at 1.2 K is $\lambda_\perp = 0.0041$ mm—as will be derived later—and amounts to $\simeq 1\%$ of the corresponding sample dimension. The value of the penetration depth, for a field oriented perpendicular to the *a-b* plane, but penetrating along the plane is $\lambda_\parallel = 0.000\,51$ mm at $T = 1.2$ K. Consequently, in the orientation $\mathbf{H}\parallel a$-b plane, where the penetration depth is bigger, the magnetic transition is expected to be broader than in the orientation $\mathbf{H}\perp a$-b plane.

Applying the anisotropic effective-mass model (within the framework of the Ginzburg-Landau theory) to our data of H_{c2} of β-(ET)$_2$ AuI$_2$, the superconducting coherence lengths $\xi_\perp$ and $\xi_\parallel$ (perpendicular and parallel to the *a-b* plane, assuming isotropic behavior within the *a-b* plane) can be calculated from

$$H_{c2\perp}(0) = \frac{\phi_0}{2\pi\xi_\parallel^2(0)} \tag{1}$$

and

$$H_{c2\parallel}(0) = \frac{\phi_0}{2\pi\xi_\perp(0)\xi_\parallel(0)} , \tag{2}$$

where ϕ_0 is the flux quantum. For β-(ET)$_2$AuI$_2$ we thus obtain $\xi_{\parallel}(0)=249\,\text{Å}$ and $\xi_{\perp}(0)=19.2\,\text{Å}$. From the relations

$$\kappa=\sqrt{1/2}H_{c2}/H_c \ , \tag{3}$$

$$\kappa=\sqrt{1/2}\frac{H_c}{H_{c1}}(\ln\kappa+0.497) \ , \tag{4}$$

both the Ginzburg-Landau parameter κ and the thermodynamical critical field H_c can be calculated. Again for β-(ET)$_2$AuI$_2$ at $T=1.2$ K we obtain for $\mathbf{H}\perp ab$, $\kappa_{\perp ab}=16.6\pm2$, $H_c=145\pm10$ Oe; and for $\mathbf{H}\parallel\mathbf{a}$, $\kappa_{\parallel a}=177\pm15$, $H_c=176\pm15$ Oe. H_c is a thermodynamical quantity which is independent of a special crystallographic orientation, in satisfactory agreement with our results. The following equations relate H_c to the temperature T, the superconducting gap Δ and the density of states at the Fermi level $N(\varepsilon_F)$:

$$H_c(T)=H_c(0)\left[1-\left[\frac{T}{T_c}\right]^2\right] \tag{5}$$

and

$$\frac{H_c^2(0)}{8\pi}=1.09\frac{\Delta^2(0)}{2}N(\varepsilon_F) \ . \tag{6}$$

Assuming a BCS-like gap $\Delta(0)=1.76k_BT_c$, where k_B is the Boltzman factor, and taking $N(\varepsilon_F)=1.67$ states/(eV molecule), a value that has been calculated for β-(ET)$_2$I$_3$ (Ref. 23) and which should approximately be the same for β-(ET)$_2$AuI$_2$, we derive from Eqs. (5) and (6) that H_c (1.2 K)$=160$ G, thus confirming the thermodymamical consistency of our H_{c1} and H_{c2} data. It is important to realize that our thermodynamic analysis is only consistent with the assumption of a weak-coupling BCS gap. Our results are not obviously consistent with the recent tunnelling experiments[24] which claim a strong-coupling gap up to four times the BCS value. This discrepancy needs to be resolved by further experiments but it is hard to see how our thermodynamic argument can be wrong.

A similar analysis for β-(ET)$_2$IBr$_2$ of H_{c1} and H_{c2}, where the H_{c2} data are taken from resistive transitions,[16] yields the following results at $T=0.5$ K: for $\mathbf{H}\perp ab$; $\kappa_{\perp ab}=10.5\pm1.5$, $H_c=87\pm10$ Oe; and for $\mathbf{H}\parallel(110)$, $\kappa_{\parallel(100)}=143\pm20$, and $H_c=144\pm20$ Oe and $H_c(0.5\text{ K})=103$ Oe, calculated from Eqs. (5) and (6) [again using a value of $N(\varepsilon_F)$ calculated for β-(ET)$_2$I$_3$]. In this case the agreement between the derived and calculated values of H_c is not quite as good as in the case of β-(ET)$_2$AuI$_2$, which could be due to pinning effects enhancing H_{c1} or could result from an error in the linear extrapolation of $H_{c2}(T)$ to $T=0.5$ K since data of the upper critical field of β-(ET)$_2$IBr$_2$ are only reported above 1.6 K.[16]

The penetration depths parallel and perpendicular to the a-b plane can be obtained from the relations (7) and (8):

$$\kappa_{\perp}=\frac{\lambda_{\parallel}}{\xi_{\parallel}} \tag{7}$$

and

$$\kappa_{\parallel}=\frac{(\lambda_{\parallel}\lambda_{\perp})^{1/2}}{(\xi_{\parallel}\xi_{\perp})^{1/2}} \ . \tag{8}$$

The above-mentioned values of $\lambda_{\parallel}$ and $\lambda_{\perp}$ at $T=1.2$ K were thus calculated; appropriate values of $\xi_{\parallel}$ and $\xi_{\perp}$ were inferred from the $H_{c2}(T)$ data via relations (1) and (2).

V. SUMMARY

We have shown by low-field magnetization measurements that ambient pressure superconductivity of β-(ET)$_2$IBr$_2$ and β-(ET)$_2$AuI$_2$ is a property of the volume of the sample. The different behavior of the magnetic transition curves for fields applied parallel and perpendicular to the crystallographic a-b plane can qualitatively be explained with the anisotropy of the London penetration depth $\lambda_{\perp}/\lambda_{\parallel}$, the macroscopically large value of $\lambda_{\perp}$, and the anisotropy of the coherence length ξ. The critical field data, H_{c1} and H_{c2}, yield a thermodynamically consistent picture when analyzed within the anisotropic effective-mass model of the Ginzberg-Landau theory with a weak-coupling BCS gap.

ACKNOWLEDGMENT

H. Schwenk thanks IBM Germany for financial support through the IBM World Trade Program.

---

[*] Present address: Walther-Meissner-Institute für Tieftemperaturforschung, D-8046 Garching, Federal Republic of Germany.

[†] Present address: IBM T. J. Watson Research Center, Yorktown Heights, N.Y. 10598.

[1] For a review, see P. M. Chaikin and R. L. Greene, Physics Today **39** (5), 24 (1986).

[2] S. S. P. Parkin, E. M. Engler, R. R. Schumaker, R. Lagier, V. Y. Lee, J. Voiron, K. Carneiro, J. C. Scott, and R. L. Greene, Phys. Rev. Lett. **50**, 270 (1983).

[3] E. B. Yagubskii, I. F. Shchegolev, V. N. Laukhin, P. A. Kononovich, M. V. Kartsovnik, A. V. Zvarykina, and L. I. Buravov, Pis'ma Zh. Eksp. Teor. Fiz. **39**, 12 (1984) [JETP Lett. **39**, 12 (1984)].

[4] J. M. Williams, H. H. Wang, M. A. Beno, T. J. Emge, L. M. Sowa, P. T. Copps, F. Behroozi, K. D. Carlson, and G. W. Crabtree, Inorg. Chem. **23**, 3839 (1984).

[5] H. H. Wang, M. A. Beno, U. Geiser, M. A. Firestone, K. S. Webb, L. Nunez, G. W. Crabtree, K. D. Carlson, J. M. Williams, L. J. Azevedo, J. F. Kwak, and J. E. Schirber, Inorg. Chem. **24**, 2466 (1985).

[6] V. N. Laukhin, E. E. Kostyuchenko, Yu V. Sushko, I. F. Shchegolev, and E. B. Yagubskii, Pis'ma Zh. Eksp. Teor. Fiz. **41**, 68 (1985) [JETP Lett. **41**, 81 (1985)].

[7] K. Murata, M. Tokumoto, H. Anzai, H. Bando, G. Saito, K. Kajimara, and T. Ishiguro, J. Phys. Soc. Jpn. **54**, 2084 (1985).

[8] H. Veith, C. -P. Heidmann, F. Gross, A. Lerf, K. Andres, and D. Schweitzer, Solid State Commun. **56**, 1015 (1985).

[9] F. Creuzet, D. Jerome, D. Schweitzer, and H. J. Keller, Europhys. Lett. **1**, 461 (1986).

[10] V. B. Ginodman, A. V. Gudenko, I. I. Zasavitskii, and E. B. Yagubskii, JETP Lett. **42**, 472 (1986).

[11] H. Schwenk, C. -P. Heidmann, F. Gross, E. Hess, K. Andres, D. Schweitzer, and H. J. Keller, Phys. Rev. B **31**, 3138 (1985).

[12] C. -P. Heidmann, H. Veith, K. Andres, H. Fuchs, K. Polborn, and E. Amberger, Solid State Commun. **57**, 161 (1986).

[13] G. A. Bowmaker and S. Hacobian, Aust. J. Chem. **21**, 551 (1968).

[14] P. Braunstein and R. J. H. Clark, J. Chem. Soc., Dalton, Trans. (1973), p. 1845.

[15] H. Schwenk, K. Andres, and F. Wudl, Solid State Commun. **49**, 723 (1984).

[16] M. Tokumoto, H. Anzai, H. Bando, G. Saito, N. Kinoshita, K. Kajimura, and T. Ishiguro, J. Phys. Soc. Jpn. **54**, 1669 (1985).

[17] M. Tokumoto, K. Murata, H. Bando, H. Anzai, G. Saito, K. Kajimura, and T. Ishiguro, Solid State Commun. **54**, 1031 (1985).

[18] V. B. Ginodman, A. V. Gudenko L. N. Zherikhina, Pis'ma Zh. Eksp. Teor. Fiz. **41**, 41 (1985) [JETP Lett. **41**, 49 (1985)].

[19] M. Tokumoto, H. Bando, H. Anzai, G. Saito, K. Murata, K. Kajimura, and T. Ishiguro, J. Phys. Soc. Jpn. **54**, 869 (1985).

[20] R. E. Schwall, G. R. Stewart, and T. H. Geballe, J. Low Temp. Phys. **22**, 557 (1976).

[21] D. U. Gubser, W. W. Fuller, T. O. Poehler, M. Lee, D. Cowan, R. S. Potember, L. -Y. Chiang, and A. Bloch, Phys. Rev. B **24**, 478 (1981).

[22] H. Schwenk, K. Andres, F. Wudl, and E. Aharon-Shalom, Solid State Commun. **45**, 767 (1983).

[23] P. Grant (private communication).

[24] M. E. Hawley, K. E. Gray, B. D. Terris, H. H. Wang, K. D. Carlson, and J. M. Williams (unpublished).